From planar boron clusters to borophenes and metalloborophenes

Article *in* Nature Reviews Chemistry · September 2017

DOI: 10.1038/s41570-017-0071

CITATIONS
174

READS
920

6 authors, including:

Wan-Lu Li
University of California, Berkeley
76 PUBLICATIONS **2,291** CITATIONS
SEE PROFILE

Tian Jian
Lawrence Berkeley National Laboratory
46 PUBLICATIONS **1,822** CITATIONS
SEE PROFILE

Tengteng Chen
Brown University
35 PUBLICATIONS **1,148** CITATIONS
SEE PROFILE

Jun Li
Tsinghua University
624 PUBLICATIONS **49,920** CITATIONS
SEE PROFILE

From planar boron clusters to borophenes and metalloborophenes

Wan-Lu Li, Xin Chen, Tian Jian, Teng-Teng Chen, Jun Li and Lai-Sheng Wang

Abstract | Elemental boron and its compounds exhibit unusual structures and chemical bonding owing to the electron deficiency of boron. Joint photoelectron spectroscopy and theoretical studies over the past decade have revealed that boron clusters possess planar or quasi-planar (2D) structures up to relatively large sizes, laying the foundations for the discovery of boron-based nanostructures. The observation of the 2D B_{36} cluster provided the first experimental evidence that extended boron monolayers with hexagonal vacancies were potentially viable and led to the proposition of 'borophenes' — boron analogues of 2D carbon structures such as graphene. Metal-doping can expand the range of potential nanostructures based on boron. Recent studies have shown that the CoB_{18}^- and RhB_{18}^- clusters possess unprecedented 2D structures, in which the dopant metal atom is part of the 2D boron network. These doped 2D clusters suggest the possibilities of creating metal-doped borophenes with potentially tunable electronic, optical and magnetic properties. Here, we discuss the recent experimental and theoretical advances in 2D boron and doped boron clusters, as well as their implications for metalloborophenes.

Boron exists in a large number of unusual chemical structures, both in its elemental form and its many chemical compounds[1], as a direct consequence of its electron deficiency. The discoveries of exciting carbon nanostructures, such as fullerenes[2], nanotubes[3] and graphenes[4], suggested the attractive prospect that boron — carbon's lighter neighbour — could form similar structures. Like carbon, boron can form exceptionally strong homonuclear covalent bonds, which are reflected in the super-hard character of almost all boron polymorphs[5]. Boron nanotubes made of triangular boron sheets were, in fact, proposed shortly after carbon nanotubes were discovered[6,7]. However, computational studies suggested that triangular planar boron lattices with hexagonal vacancies were more stable and more suitable to form the putative boron nanotubes[8,9]. The proposed B_{80} fullerene featured pentagonal vacancies[10], which might explain why it is a much higher-energy isomer than the various low-symmetry structures of the core–shell type[11–14]. A systematic understanding of the geometric structures and chemical bonding of size-selected boron clusters, and of their evolution as a function of size, is clearly an essential foundation for the discovery of new boron-based nanostructures. This, however, has proved to be a challenge that has required more than a decade of sustained joint experimental and theoretical investigation[15–17].

Neutral clusters are generally more difficult to study because mass spectrometric techniques, necessary for cluster size selection, require charged particles. Small boron cluster cations were first produced and their fragmentation and chemical reactivity were studied in the late 1980s[18–21], but no structural and spectroscopic information was available until 2002, when photoelectron spectroscopy (PES) was combined with quantum chemistry to investigate size-selected boron clusters[22]. Since then, PES in conjunction with high-level *ab initio* calculations has become an effective means to probe the electronic structure and chemical bonding of boron clusters[22–39]. Size-selected anionic boron clusters are extremely interesting, as even fairly large clusters have been found to be planar or quasi-planar (2D)[22–39]. Although bulk boron is characterized by 3D polyhedral structural features[5,40,41], early theoretical calculations suggested that the isolated B_{12} icosahedron — the dominant motif in bulk boron — was less stable than 2D structures[42,43]. The higher stability of 2D structures can be ascribed to the electron-deficient character of boron and its propensity to form multi-centred chemical bonds[1]. Chemical bonding analyses based on the adaptive natural density partitioning (AdNDP) method[44] revealed that all 2D boron clusters consist of an outer ring featuring strong two-centre, two-electron (2c–2e) B–B bonds (in which two valence electrons are shared between two atoms) and one or more inner atoms interacting with the peripheral ring almost exclusively through delocalized σ and π bonding[15–17,45]. The electron delocalization has an important role in stabilizing the 2D structures, giving rise to concepts of σ and π aromaticity and antiaromaticity according to Hückel's rule[15–17,25,45–47]. Recent investigations have shown that even larger anionic boron clusters, including those comprising over 30 atoms, preferentially adopt planar structures[48–50]. Even the minimum-energy structure of B_{40}^- — the largest experimentally characterized boron cluster — corresponds to a 2D arrangement of the atoms[51], although 3D borospherene B_{40}^- is also an energetically accessible isomer. By contrast, for a neutral cluster of the same size, B_{40}, borospherene is the most stable structure[51].

Notably, the discovery of the planar hexagonal B_{36} cluster provided the first experimental evidence for the viability of monolayer boron, which was named borophene[48]. The B_{35}^- cluster with two adjacent hexagonal vacancies provided an even more flexible motif for borophenes[49]. The double hexagonal vacancies in B_{35}^- result in an asymmetric cluster, enabling borophenes with different hole densities and orientations to be constructed. Earlier experimental and theoretical characterizations of boron clusters were reviewed in 2006 (REF. 15), and a brief account addressing the structural fluxionality and chemical bonding appeared in 2014 (REF. 16). Recently,

a more comprehensive review that includes the progress made over the past decade on the characterization of size-selected boron clusters using PES and computational chemistry has been published[17].

The structures and properties of boron clusters can be further tuned by doping with metal atoms, considerably expanding the plethora of possible boron-based nanostructures. A series of aromatic borometallic molecular wheels with a highly coordinated central transition metal atom, M, inside a monocyclic boron ring (designated as M©B_n^-) has been produced and characterized for $n = 8–10$ (REFS 52–56). Very recently, larger doped boron clusters, CoB_{16}^- and MnB_{16}^-, have been observed to feature unprecedented tubular (or drum-like) structures[57,58]. A low-lying TaB_{20}^- drum isomer of perfect D_{10d} symmetry has also recently been found[59]. The discoveries of 2D CoB_{18}^- and RhB_{18}^- clusters, in which planar boron lattices are doped by the transition metal atoms, were surprising, opening up the possibility of metallo-borophenes[60,61]. In the meantime, properties of hypothesized metalloborophenes that contain other transition metals, such as iron and manganese, have also been studied computationally[62–65]. The recent syntheses and characterization of borophenes on silver substrates[66,67] make the idea of synthesizable metalloborophenes conceivable, opening the door to a new class of 2D materials with tunable chemical and physical properties. In this Perspective, we discuss the exciting advances in the studies of size-selected boron and doped boron clusters and, in particular, the findings of planar CoB_{18}^- and RhB_{18}^- and their implications for metalloborophenes.

Planar boron clusters

Medium-sized boron clusters

FIGURE 1 summarizes the global minimum structures of B_n^- for $n = 3–30$ and $35–38$, confirmed from careful comparison between PES and theoretical studies. These results represent a sustained and systematic joint experimental and theoretical effort, spanning more than a decade from the first study in 2002 (REF. 22) to the very recent resolution of the structures of B_{37}^- and B_{38}^- (REF. 50). The minimum-energy structures of the boron cluster monoanions are presented in FIG. 1, but, in some cases, energetically accessible isomers exist. When a low-energy isomer is energetically close to the minimum-energy isomer, the two may coexist at finite temperatures, and they can be observed experimentally in different ratios. For example, the majority of the most stable structures are 2D, but in the cases of B_{28}^- and B_{29}^-, small amounts of 3D borospherene isomers have been observed to coexist with the 2D structures[37,38,68]. Note that some of the 2D structures shown in FIG. 1 are quasi-planar; for example, both B_7^- and B_{12}^- have bowl-shaped structures[25,26]. The distortion is due to the peripheral B–B bonds being stronger and shorter than the internal bonds, causing slight out-of-plane migration of the interior atoms. This explanation was confirmed by substituting a peripheral boron atom with a larger valence-iso-electronic atom, aluminium. The resulting AlB_6^- and AlB_{11}^- clusters were indeed found to be planar because the longer Al–B bonds expanded the size of the outer ring[69].

Neutral boron clusters are considerably more challenging to study experimentally, owing to the difficulty in cluster size discrimination. Charged clusters can be conveniently detected and size-selected by mass spectrometry, whereas neutral clusters require more sophisticated experimental techniques. For example, IR spectra of B_{11}, B_{16} and B_{17} were measured using an IR–UV double resonance approach, and these neutral clusters were all found to have structures similar to those of the most energetically stable corresponding anions[70]. Neutral spectroscopic information can also be obtained from PES of the corresponding anions. In particular, high-resolution PES of negatively charged clusters can

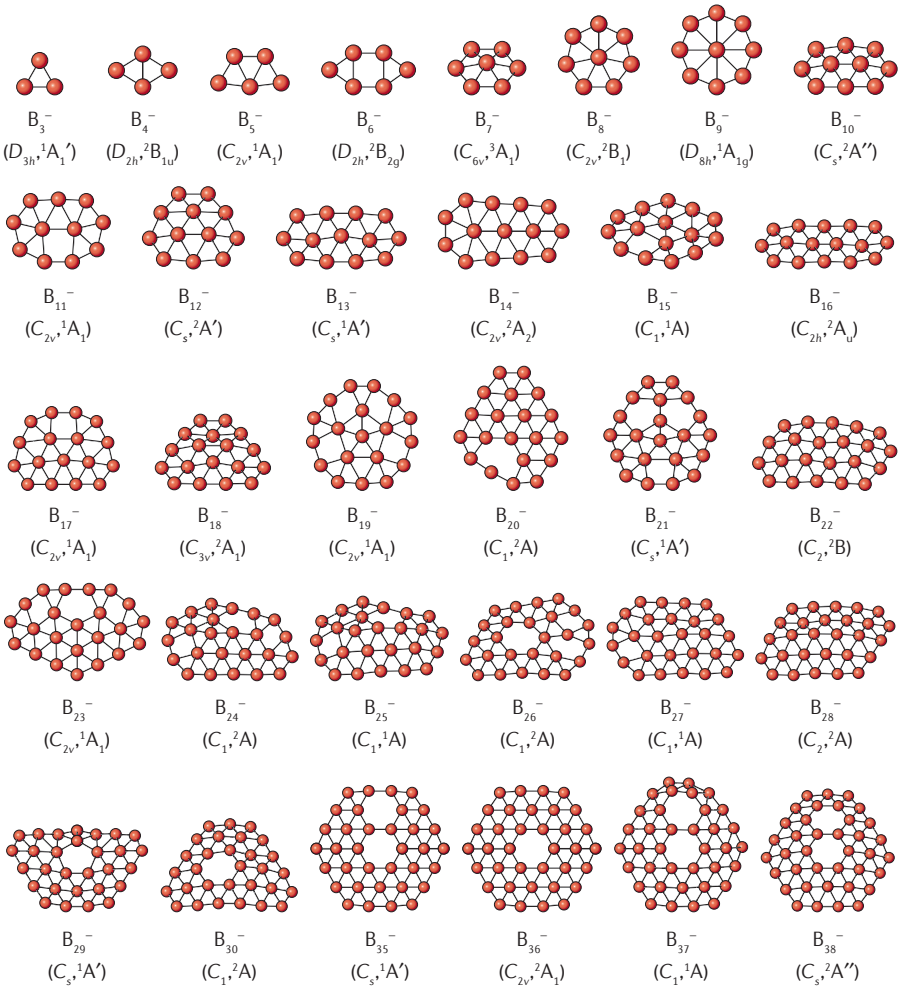

Figure 1 | **Structures of size-selected boron clusters.** Summary of the minimum-energy structures, point group symmetries and electronic states of B_n^- clusters ($n = 3–30$ and $35–38$) resulting from joint photoelectron spectroscopy and theoretical studies[17,39,50]. The dominant feature of boron clusters is their tendency to form planar or quasi-planar (2D) structures, in which bonding electrons are shared or delocalized within the 2D plane, as a result of the electron deficiency of boron. Triangles of B_3 are characteristic of borane compounds in boron chemistry. However, tetragonal, pentagonal and hexagonal vacancies appear in the bare 2D boron clusters with increasing cluster size. The hexagonal vacancy was first discovered in B_{36}^-, providing experimental evidence for the viability of monolayer boron with hexagonal vacancies and leading to the proposition of borophene[48].

yield vibrational information about the corresponding neutral final states. Very recently, a high-resolution PES study of B_{11}^- and B_{12}^- using photoelectron imaging has resolved several vibrational modes for the corresponding neutral B_{11} and B_{12} clusters, confirming that their 2D structures are similar to the parent anions[71].

The structures of a series of B_n^+ cationic clusters for $n = 12–25$ were investigated using ion mobility experiments in combination with density functional theory (DFT) calculations[72]. The structures of B_{12}^+ and B_{15}^+ were found to be similar to those of the corresponding anions (FIG. 1). Anionic B_{13}^- and B_{14}^- have elongated 2D structures (FIG. 1) because they are antiaromatic (each with eight π electrons) according to Hückel's rule[25]. However, the structures of B_{13}^+ and B_{14}^+ were found to be more circular, consistent with previous calculations[73,74]. A major departure of the structures of the cationic clusters from those of the 2D anions (FIG. 1) was reported for $n = 16$, beyond which ($n = 16 – 25$) tubular structures were deduced[72]. Very recently, the IR spectrum of B_{13}^+ has been reported[75], confirming its circular structure and its structural dynamicity[76].

The structures of B_{36}^- and B_{35}^-

Beyond $n = 30$, the B_{36}^- cluster gives a characteristic photoelectron spectrum displaying an unusually low electron binding energy[17,48]. The minimum-energy structure for B_{36}^- was found to have pseudo-C_{6v} symmetry (only slightly distorted relative to C_{2v}) with a central hexagonal vacancy (FIG. 1) not observed in other known structures previously, whereas neutral B_{36} was found to have C_{6v} symmetry.

The hexagonal B_{36} cluster and the concept of borophene. Boron cannot form graphene-like hexagonal layers because of its electron deficiency. Boron sheets consisting of B_3 triangles, which are obtained by incorporating a boron atom in the centre of the hexagon of a graphene-like boron structure, were originally used to form the hypothesized boron nanotubes[6,7]. However, such triangular lattices are too electron-rich, so that out-of-plane distortions occur, leading to rippled boron layers according to subsequent computational investigations[77–80]. Further theoretical studies suggested that a triangular lattice with periodic hexagonal vacancies would be truly planar and much more stable than a close-packed triangular lattice[8,9]. The hexagonal vacancy found in the B_{36} cluster[48] is reminiscent of the hexagonal vacancies in the predicted 2D boron sheets[8,9]. The proposed 2D boron structure based on the B_{36} cluster (shown in FIG. 2a) exhibits a hexagonal hole density of $\eta = 1/27$ (one vacancy for every 27 triangular lattice sites)[8]. Therefore, the hexagonal B_{36} cluster can be considered as the repeated motif of an extended boron-monolayer with hexagonal vacancies, in analogy with the hexagonal C_6 motif in graphene. The B_{36} cluster thus provides indirect experimental evidence for the viability of monolayer boron with hexagonal vacancies. The name 'borophene' was coined to designate this class of new boron nanostructures in analogy to graphene[48].

B_{35}^- as a more flexible motif for borophenes. The photoelectron spectrum of B_{35}^- was well resolved and displayed some similarity to that of B_{36}^-, suggesting that the minimum-energy structure of B_{35}^- might be related to the structure of B_{36}^- (REF. 49). Minimum-energy structure searches identified the most stable structure of B_{35}^- to be quasi-planar with a double-hexagonal vacancy (FIG. 1), which can be obtained by simply removing a boron atom from the interior plane of pseudo-C_{6v} B_{36}^-. The simulated photoelectron spectrum of B_{35}^- was in remarkable agreement with experiment, providing firm confirmation of the stability of the quasi-planar structure found for B_{35}^-. It turned out that the hexagonal B_{35} cluster can be an even more flexible building block for constructing borophenes (shown schematically in FIG. 2b,c)[49]. Other arrangements of the B_{35} clusters are also possible, creating borophenes with different hole patterns and densities, many of which have been considered computationally[81,82]. The double hexagonal vacancy seems to be a common structural feature in large 2D boron clusters; it was also found in the recently reported B_{37}^- and B_{38}^- clusters[50] (FIG. 1), as well as in the low-energy 2D B_{40}^- isomer[51].

Experimental syntheses of borophenes on inert substrates. Boron does not exist in any bulk allotropes with layered structures, so experimental production of borophenes would have to rely on nucleation and growth on chemically inert substrates; a vacuum environment or inert atmosphere would be required to avoid oxidation or other inadvertent reactions of the nascent borophenes. Hence, it is not surprising that the first considerations of the formation of borophenes were purely theoretical[83–85]. Initial studies of borophenes on silver or copper substrates predicted the β_{12} structure[81], which consists of rows of hexagonal vacancies similar to the structure shown in FIG. 2c, to be the most stable[85]. In a recent major advance in the experimental synthesis, borophenes were grown on a Ag(111) surface and their structures characterized by using both scanning tunnelling microscopy and transmission electron microscopy[66]. Even with these high-resolution methods, the atomic structures were not fully resolved, but comparison between simulated images and experiment suggested that the synthesized borophenes have a corrugated triangular lattice. Subsequent experimental and theoretical investigations concluded that the synthesized borophenes on

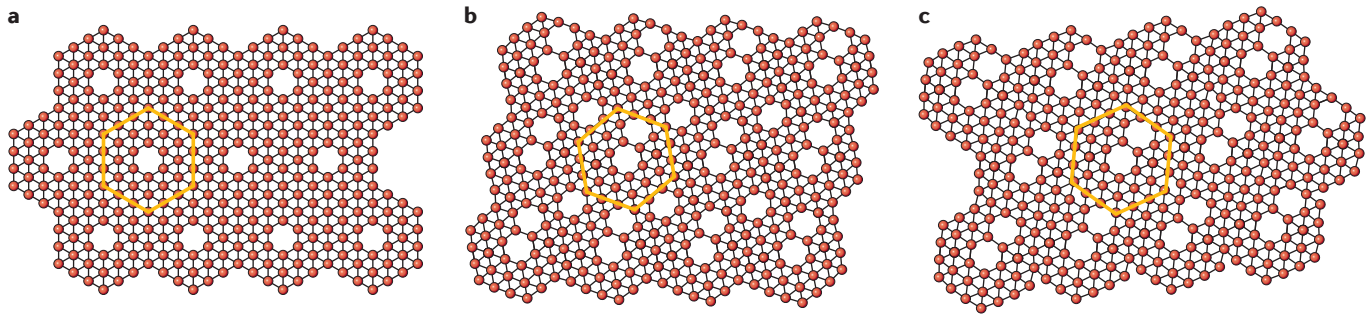

Figure 2 | **Borophenes.** Two-dimensional boron clusters with hexagonal vacancies can be viewed as motifs to produce borophenes with different hole densities and hole patterns. The yellow frame highlights the single unit structure that is periodically repeated in two dimensions. **a** | Borophene formed from B_{36} (REF. 48). **b** | Borophene formed from B_{35} (REF. 49). **c** | Borophene formed from B_{35} with a different hole pattern[49].

Ag(111) are likely to have the β_{12} and χ_3 structures[67,86,87], which both feature hexagonal vacancies[81]. These conclusions are in line with theoretical calculations, which suggest that borophenes with hexagonal vacancies are more stable than those presenting a close-packed and corrugated triangular lattice both in free-standing layers[8,9,81,82] and on silver substrates[85–89]. An interesting substrate-induced undulation of the β_{12} borophene on Ag(111) was recently predicted and observed experimentally[87]. The rippled configuration of the borophene atomic structure results from the surface morphology of the substrate and suggests potential for increased mechanical flexibility. Borophenes represent a new class of 2D materials with many interesting potential properties, such as graphene-like metallic character as Dirac fermion charge carriers, excellent elasticity with ideal mechanical strength[88–92] and relatively high-temperature superconductivity[93–96].

Metal-doped boron clusters

Doping boron clusters with metal atoms provides a means to expand the potential nanostructures that can be constructed from boron. Unlike valence-perfect carbon, the electron deficiency of boron implies that its clusters would be much more susceptible to metal doping, potentially leading to new structures, bonding and tunable properties. Several metal-doped boron clusters have been characterized by joint PES and computational studies, from the metal-centred borometallic wheels (MB_n^-, $n=8–10$)[52–56] to sandwich-type clusters[97–103] and drum-type structures[57–59] (FIG. 3). In particular, the recent observation of the planar CoB_{18}^- and RhB_{18}^- clusters with the metal dopant as a part of the 2D boron network suggests the tangible possibility of metalloborophenes[60,61].

Small metal-doped boron clusters MB_n^-

Inspired by the highly symmetric doubly aromatic B_9^- boron wheel or $B©B_8^-$, which consists of a central boron atom in a B_8 ring[24] (FIG. 1), a design principle was proposed in which the central boron atom would be replaced by a metal atom to create similar doubly aromatic borometallic clusters[52,104]. Initially, a series of highly stable transition metal-centred monocyclic boron rings MB_n^- (with $n=8–10$) were produced[52–56], including the record 10-coordinated tantalum and niobium for 2D systems[54] (FIG. 3). Subsequently, larger CoB_{12}^- and RhB_{12}^- clusters were found to exist in half-sandwich-type structures with the quasi-planar B_{12} moiety coordinated to the metal atom[100] (FIG. 3). The FeB_{14}^- and FeB_{16}^- clusters were studied computationally and predicted to be arranged in drum-type structures[105,106]. The first doped drum-type boron clusters to be investigated jointly by PES and theoretical calculations were CoB_{16}^- and MnB_{16}^-, which were found to be characterized by two B_8 moieties sandwiching the central metal atom[57,58] (FIG. 3). Very recently, another joint PES and theoretical study has shown that the TaB_{20}^- cluster possesses two close-lying isomers: a B_2-capped-TaB_{18}^- drum-type structure and an unprecedented D_{10d}-TaB_{20}^- drum structure with a record 20-coordinated tantalum atom[59] (FIG. 3).

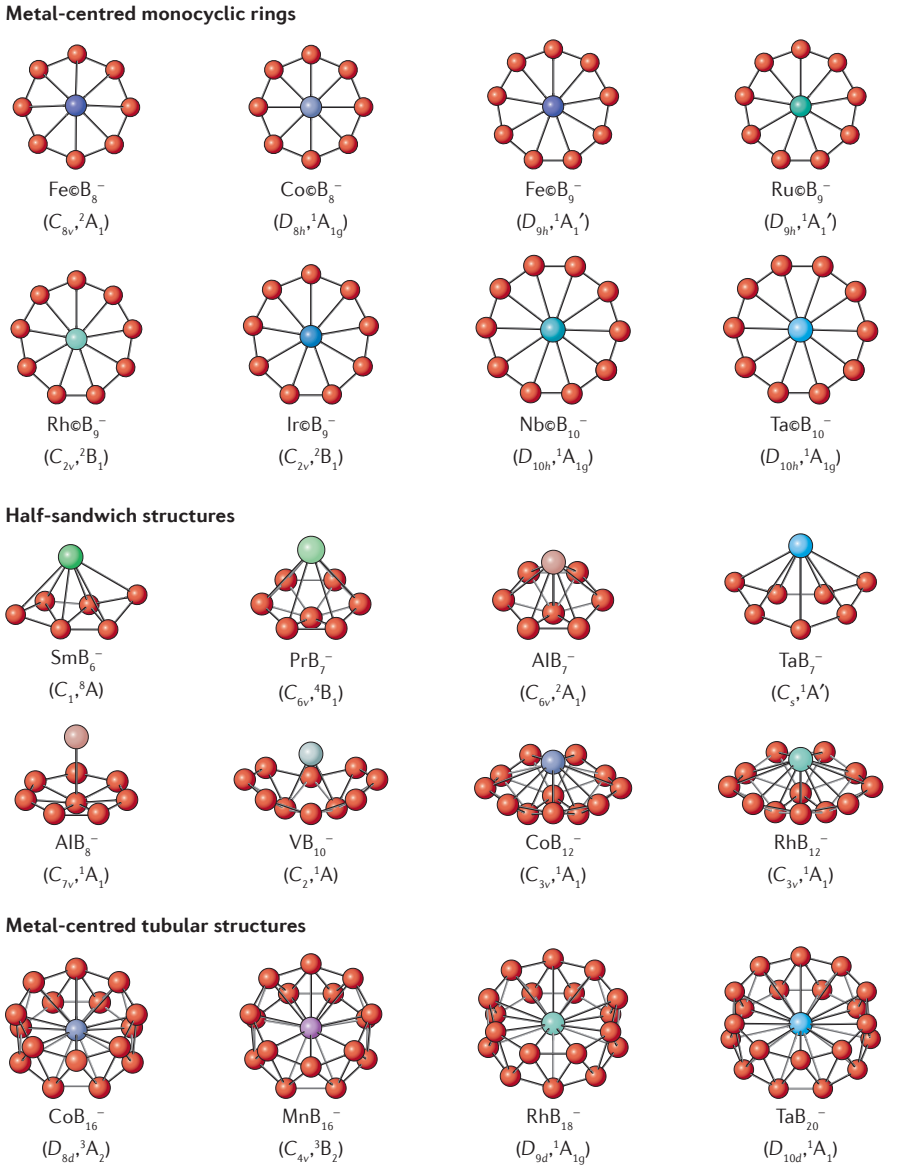

Figure 3 | **Metal-doped boron clusters.** Metal-centred monocyclic rings[52–56], half-sandwich type structures[97–103] and metal-centred tubular structures[57–59] are three classes of metal-doped boron clusters that have been observed experimentally. For each structure, the point group symmetry and electronic state are reported.

The most surprising observation was the Co-doped B_{18}^- cluster, CoB_{18}^-, which was investigated by means of PES and *ab initio* calculations[60]. A drum-type structure similar to CoB_{16}^- was expected, but instead a perfect 2D structure was found, in which the cobalt atom became an integral part of the planar boron network. Subsequently, the RhB_{18}^- cluster was found to exist in two isoenergetic structures[61]: a drum isomer (FIG. 3) and a 2D structure similar to that of CoB_{18}^-. These relatively large 2D doped boron clusters with the metal dopants as a part of the 2D boron cluster are unprecedented. The analyses of their structures and bonding suggest that infinitively large boron monolayers decorated

with metal dopants, that is, metallo-borophenes, are potentially viable. These recent findings and their implications for metalloborophenes constitute the impetus for this Perspective and are the main focus in the following.

Cobalt as an integral part of CoB_{18}^-

FIGURE 4a shows the 193 nm photoelectron spectrum of CoB_{18}^-, which revealed extremely high electron binding energies compared with CoB_{16}^-, suggesting that CoB_{18}^- is an electronically stable system. Searches for minimum-energy structures using the Tsinghua Global Minimum (TGMin) method, which is based on a basin-hopping algorithm[107,108], in combination with high-level calculations found that the most stable structure of the CoB_{18}^- cluster is perfectly planar with C_{2v} symmetry (insert, FIG. 4b). Conversely, the putative drum-shaped structure (insert, FIG. 4c) was found to be a much higher-energy isomer. The simulated spectrum for the planar structure (FIG. 4b) agrees well with the experimental spectrum, as opposed to those simulated for other low-energy isomers[60], providing firm evidence that the identified 2D CoB_{18}^- isomer is the most stable.

The cobalt atom in 2D CoB_{18}^- is bonded to seven boron atoms in its first coordination shell, different from the Co©B_8^- borometallic wheel[52] (FIG. 3). In Co©B_8^-, the peripheral B–B distances are relatively short and an eight-atom ring is necessary to accommodate the cobalt atom, which is bonded to the boron ring through delocalized covalent bonding[52]. In the planar CoB_{18}^- cluster, the interior B–B bonds around the cobalt atom are slightly longer; hence, a seven-atom ring creates enough room to accommodate cobalt. In fact, the cobalt atom in CoB_{18}^- is an integral part of the boron network with strong covalent interactions. The binding energy between the cobalt atom and the B_{18} host is calculated to be 162 kcal mol^{-1}, indicating the potential thermodynamic stability of CoB_{18}^-. Chemical bonding analyses using the AdNDP method[44] (FIG. 4d) indicate that the $3d_{z2}$, $3d_{xz}$ and $3d_{yz}$ orbitals of cobalt remain nearly doubly occupied as lone pairs (occupation number, ON = 1.83–1.99 |e|); hence, there are only very weak π–π interactions between cobalt and boron. The cobalt atom interacts with the surrounding seven boron atoms mainly through the six 4c–2e delocalized σ bonds (ON = 1.96 |e|) (FIG. 4d). In addition to the thirteen localized 2c–2e peripheral B–B bonds, there are five delocalized 4c–2e σ bonds, primarily describing bonding between the inner B_7 ring and the periphery. Most interestingly, there are five delocalized π bonds with ten delocalized π electrons, which suggest unique Hückel aromaticity for the planar CoB_{18}^- cluster, similar to the bare 2D boron clusters[15–17,47].

The oxidation state of the central transition metal atom in CoB_{18}^- also deserves comment, as it is relevant to the catalytic and magnetic properties of the system. The CoB_{18}^- cluster is closed shell and thus diamagnetic. Integration of the 3*d* electrons remaining on the cobalt atom revealed a remarkably low oxidation state, cobalt(I), owing to the weak oxidizing ability or low electronegativity of boron. Conversely, the removal of an electron from the $3d_{z2}$ highest occupied molecular orbital results in a neutral, paramagnetic CoB_{18} cluster[59] and a higher oxidation state for cobalt, that is, cobalt(II). It is interesting to note that the low oxidation state of cobalt in CoB_{18}^- suggests that it would be readily oxidized, yet it exhibits a very high electron binding energy because of its closed-shell nature. The high electron binding energy may indicate possible chemical stability, which will be important for the putative metalloborophenes discussed below.

Competition between 2D and 3D RhB_{18}^-

As shown above, the cobalt atom is clearly too small to form the D_{9d} drum for CoB_{18}^-. Rhodium is below cobalt in the periodic table and is slightly bigger. So, an interesting question arises: does RhB_{18}^- favour the D_{9d} drum or a 2D structure similar to CoB_{18}^-? The photoelectron spectrum of RhB_{18}^- shows a weak feature at a low binding energy (FIG. 5a), suggesting the presence of more than one isomer[61]. Minimum-energy structure searches along with high-accuracy calculations resulted in two low-energy structures with total energies that differ by only 6 kcal mol^{-1} (REF. 61). Highly accurate

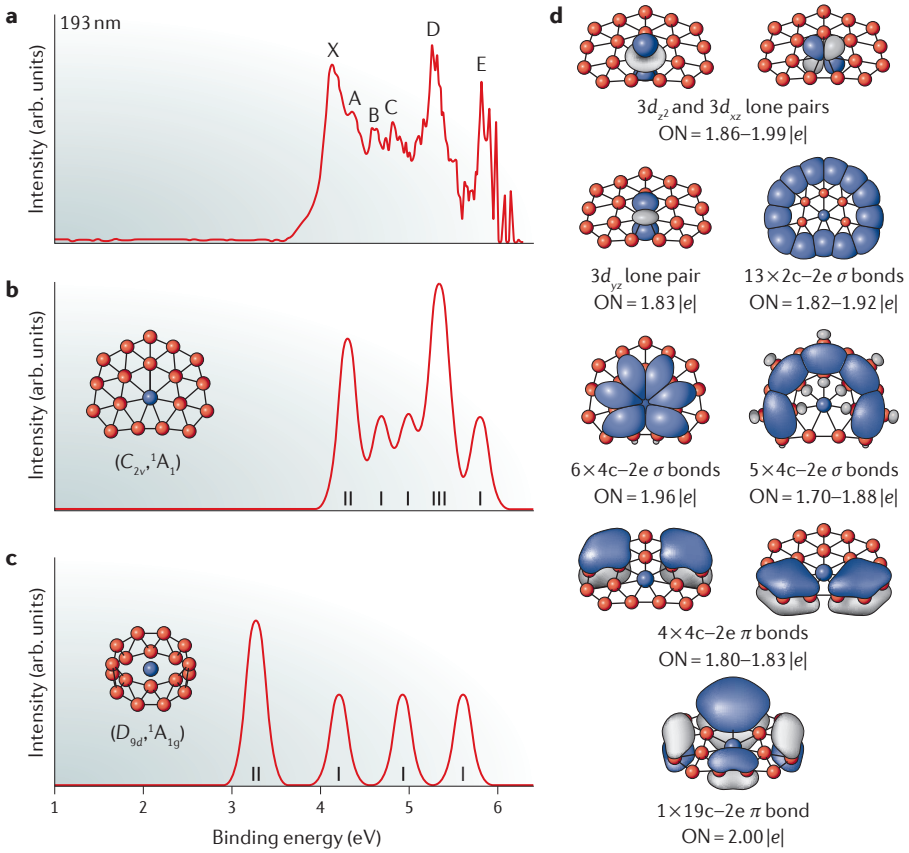

Figure 4 | **The CoB_{18}^- cluster. a** | Photoelectron spectrum of CoB_{18}^- measured at 193 nm (6.424 eV). The observed photodetachment bands are labelled with capital letters[60]. **b** | The simulated spectrum for the CoB_{18}^- minimum-energy structure corresponding to a closed shell (C_{2v}) structure (shown in inset). The vertical bars are the computed detachment transitions[60]. **c** | The simulated spectrum of a higher-energy drum-like isomer (D_{9d}) of CoB_{18}^- (shown in inset)[60]. **d** | Chemical bonding analyses for the global minimum C_{2v} structure of CoB_{18}^- using adaptive natural density partitioning[44]. Note that the five delocalized π bonds render CoB_{18}^- aromatic[60]. ON, occupation number. Adapted with permission from REF. 60, Wiley-VCH.

coupled cluster calculations (CCSD(T)) found the minimum-energy structure to be quasi-planar with C_s symmetry at finite temperatures (insert, FIG. 5b) and its simulated spectrum to agree well with the main PES features observed experimentally[61]. The D_{9d} drum structure (insert, FIG. 5c) was found to be a slightly higher-energy isomer at finite temperatures, and its simulated spectrum found to be consistent with the weak low-binding-energy signals detected experimentally[61]. The combined theoretical data for the two isomers are in good agreement with the experimental observations, providing considerable credence for the coexistence of the two isomers. As expected, the slightly larger rhodium atom does indeed stabilize the D_{9d} drum-like isomer relative to drum-like CoB_{18}^-, resulting in a smaller energy difference between the drum-like and 2D RhB_{18}^- isomers[60]. At 0 K and at the CCSD(T) level of theory, the CoB_{18}^- 2D isomer is 25 kcal mol^{-1} more stable than the drum-like isomer, whereas drum-like RhB_{18}^- is 5.29 kcal mol^{-1} more stable than the 2D isomer. However, at finite temperatures, the RhB_{18}^- 2D isomer becomes more stable because of entropic effects and is indeed the main isomer observed experimentally. Two-dimensional RhB_{18}^- is slightly different from the perfectly planar CoB_{18}^- cluster. As was observed for the $Rh©B_9^-$ and $Co©B_8^-$ borometallic wheels[53] (FIG. 3), the larger rhodium atom in 2D RhB_{18}^- requires an eight-atom first-coordination shell, which is larger than the seven-atom one required by the cobalt atom in 2D CoB_{18}^-. However, even the eight-atom coordination shell is too small for rhodium in the 2D RhB_{18}^-. This is reflected by the out-of-plane dislocation of one of the boron atoms coordinated to rhodium, which gives rise to a penta-coordinated boron atom and the overall convex shape of the 2D RhB_{18}^- cluster. Although the bonds in the B_{18}^- frameworks in RhB_{18}^- and CoB_{18}^- show some similarities — for example, both have ten π electrons with Hückel aromaticity (FIG. 5d) — the bonds between the central metal atom and the surrounding boron atoms exhibit some interesting differences. There is a fairly strong localized π bond between the rhodium atom and the buckled boron atom; there is also a localized Rh–B σ bond with the boron atom opposite the buckled atom, in addition to the delocalized σ bonds between rhodium and its first coordination shell. Overall, the rhodium atom displays quite strong covalent bonding with the surrounding eight boron atoms and, as occurs for cobalt in CoB_{18}^-, becomes an integral part of the 2D framework in planar RhB_{18}^-. Hence, despite the slight difference in bonding, both the cobalt and rhodium atoms become an integral part of the 2D boron network in their respective doped boron clusters.

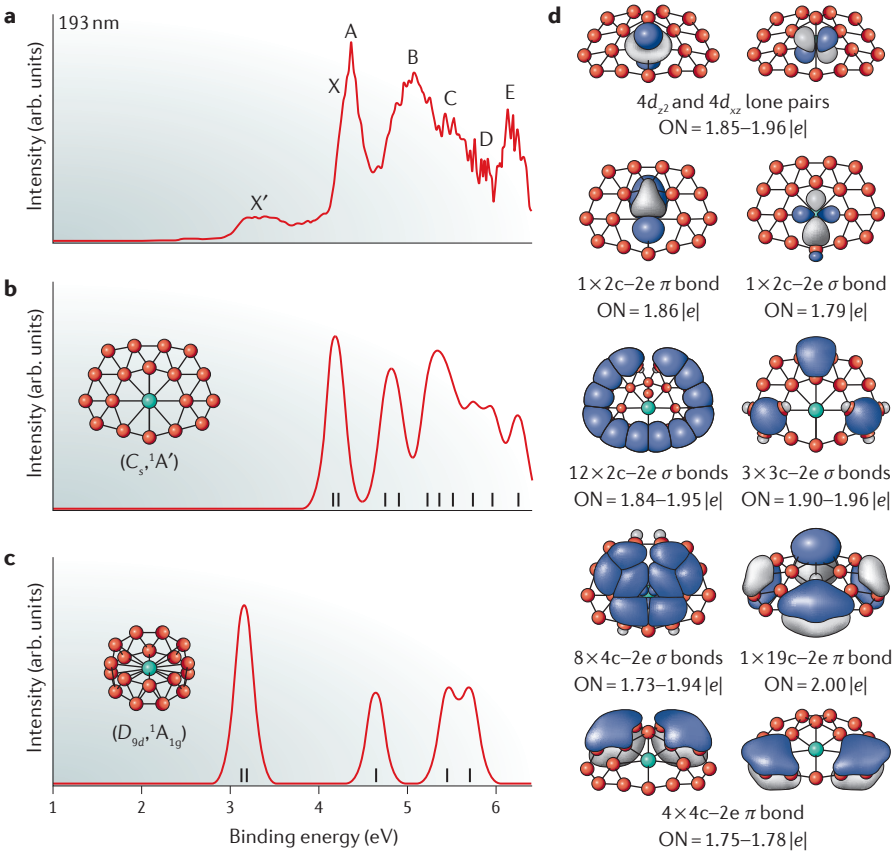

Figure 5 | **The RhB_{18}^- cluster. a** | Photoelectron spectrum of RhB_{18}^- measured at 193 nm (6.424 eV). The observed photodetachment bands are labelled with capital letters[61]. **b** | Simulated spectrum for the RhB_{18}^- minimum-energy structure corresponding to a closed-shell (C_s) structure (shown in inset). The vertical bars are the computed detachment transitions[61]. **c** | Simulated spectrum of a close-lying drum-like RhB_{18}^- isomer (D_{9d}) (shown in inset). This isomer is present experimentally as a secondary species and is responsible for the weak detachment feature X′ (REF. 61). **d** | Chemical bonding analyses for the global minimum 2D C_s structure of RhB_{18}^- using adaptive natural density partitioning[44]. Note that the five delocalized π bonds render RhB_{18}^- aromatic[61]. ON, occupation number. Adapted from REF. 61 .

2D MB_n clusters and metalloborophenes

The observation of large planar doped boron clusters, in which transition metal dopants become an integral part of the 2D boron network, suggests that infinitely large 2D boron monolayers doped with metals (that is, metalloborophenes) are potentially viable. Unlike graphene, borophenes exhibit remarkable structural diversity and flexibility with different patterns of hexagonal vacancies and densities in an otherwise planar triangular lattice (FIG. 2). The hexagonal vacancies are necessary to balance the electron distributions effectively, giving rise to the highly stable and planar boron monolayers[8,9], as opposed to the electron-rich close-packed triangular lattice, which results in corrugations and out-of-plane distortions[77–80]. Appropriate metal doping into the borophene plane has similar effects to the hexagonal vacancies, potentially creating a new class of 2D materials with tunable catalytic, magnetic and optical properties. Perfectly planar CoB_{18}^- was the first experimentally confirmed cluster in which the cobalt atom was found to be covalently bonded to the boron network and may be viewed as the unitary structure for extended metalloborophenes.

FIGURE 6a presents a schematic of an extended 2D structure formed by using the planar CoB_{18} units. The CoB_{18} motif has a hepta-coordinated Co centre; thus, pentagonal-shaped vacancies inevitably appear in a periodic arrangement. In the current case, each pentagonal-shaped vacancy consists of nine atoms, two of

which are shared between two adjacent vacancies to form a nonagonal vacancy. The nonagonal-hole density of this putative metalloborophene is one nonagonal vacancy per CoB_{18} unit. However, the RhB_{18} quasi-planar cluster can serve as a better unit structure to construct a close-packed metalloborophene sheet without any vacancies over the plane, as illustrated in FIG. 6b. Although the eight Rh–B bonds in RhB_{18} are not equivalent, an idealized eight-coordinate network is viable to form a perfectly planar or quasi-planar structure without vacancies. FIGURE 6b shows a schematic structure (not optimized) of a possible metalloborophene based on RhB_{18}, in which the corrugation is due to the quasi-planarity of the 2D RhB_{18} units. It is conceivable that perfect planar building blocks will be discovered with suitable dopants. In general, planar structural units with hexagonal or octagonal symmetries are more suitable for assembling metallo-borophenes without vacancies. Metal atoms with covalent radii smaller than cobalt may be candidates to form hexa-coordinated doped boron clusters, whereas metal atoms with covalent radii comparable to rhodium may be good candidates to form octa-coordinated doped boron clusters. With the available transition metal and lanthanide elements with different atomic sizes, electron configurations and oxidation states, it may be possible to discover metalloborophenes with tunable optical, catalytic and magnetic properties.

Iron-doped boron monolayers have recently been studied using DFT calculations[62]. Three stable iron-doped borophenes with decreasing stabilities were found, namely α-FeB_6, β-FeB_6 and γ-FeB_6. The most stable form, α-FeB_6, consists of octa-coordinated Fe (Fe©B_8) with a slight corrugation of the boron plane, similar to the model shown in FIG. 6b. The second most stable form, β-FeB_6, can be viewed as an iron atom existing in each hexagonal vacancy of the α-sheet[8]. The iron atoms are out-of-plane in the β-FeB_6 structure, because the hexagonal hole is too small to include an iron atom. The least stable γ-FeB_6 sheet is perfectly planar, consisting of a graphene-like boron layer with half of the hexagons filled with an iron atom. The α-FeB_6 monolayer is predicted to be metallic, whereas both the β-FeB_6 and γ-FeB_6 metalloborophenes are predicted to be semiconductors with considerable absorption in the visible spectral range. A more recent study[63] reports an FeB_2 metalloborophene layer, which displays linear dispersion (that is, Dirac cones) near the Fermi level. The FeB_2 layer consists of a hexagonal boron layer with an iron atom coordinated above each hexagon out of the boron plane. Another recent theoretical study[64] found a new 2D FeB_6 allotrope, *tri*-FeB_6, which essentially consists of two α-sheets sandwiching an iron layer located at each hexagonal vacancy. The *tri*-FeB_6 2D layer is found to be much more stable than the monolayer metalloborophenes, as well as having greatly enhanced in-plane stiffness with unusual negative Poisson's ratio upon oxidation. These theoretical studies provide further evidence for the viability of metalloborophenes.

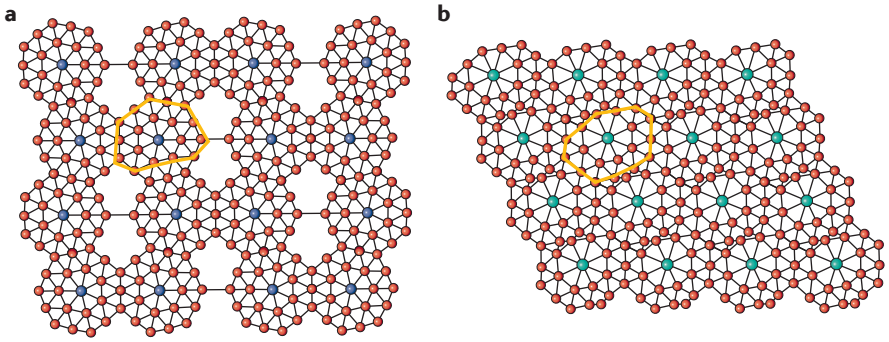

Figure 6 | **Metalloborophenes. a** | A schematic metalloborophene layer constructed from planar CoB_{18} units. **b** | A schematic metalloborophene layer constructed from quasi-planar RhB_{18} units. The yellow frame in each figure indicates the unit structure that is repeated in the two spatial dimensions. These are schematic (non-optimized) structures, showing the viability of metalloborophenes inspired by the 2D metal-doped boron clusters[60,61].

As there are no bulk metal borides containing layers of boron doped with metal atoms[109], the putative metalloborophenes potentially represent a completely new class of 2D materials following borophenes. These new nanostructures may be synthesized through similar methods to those used for the syntheses of borophenes[66,67] by introducing a desired metal component during deposition on a chemically inert substrate.

Concluding remarks and perspectives

Boron is known to be a 'rule breaker' because of its electron deficiency, resulting in chemical compounds with unusual stoichiometry and chemical bonding. Size-selected boron clusters are no exception. Through the extensive experimental and theoretical efforts of the past decade, we have discovered a remarkable structural diversity for boron clusters of different sizes. The structural scene becomes even more complicated when boron clusters are doped with metal atoms, owing to possible spin multiplicity and strong electron correlation effects. Comprehensive understanding of boron and/or metal-doped boron clusters requires state-of-the-art experimental approaches and high-level theoretical calculations to explore the potential energy landscape and mechanisms of chemical bonding. Unlike bulk boron, the boron clusters that have been investigated experimentally are mostly found to exist in stable 2D structures, even up to fairly large cluster sizes. The discovery of the planar hexagonal B_{36} cluster was a breakthrough in the study of boron clusters, giving rise to the concept of borophene and its experimental viability. Subsequent syntheses of borophenes on silver substrates have provided macroscopic samples of this new form of 2D materials, which will stimulate intense investigations into their unusual chemical and physical properties[110–113]. The recent observations of transition metal-doped 2D boron clusters (CoB_{18}^- and RhB_{18}^-) suggest the exciting possibility of metalloborophenes, which represent a new class of 2D materials with tunable chemical and physical properties. These findings have stimulated broad interest in boron clusters and nanostructures. With improving experimental sophistication and increasing computational power, it is expected that boron clusters with exotic structures and chemical bonds, or new boron-based nanostructures with tailored structures and properties, will be uncovered at an increasing pace.

Wan-Lu Li, Xin Chen and Jun Li are at the Department of Chemistry, and Key Laboratory of Organic Optoelectronics and Molecular Engineering of Ministry of Education, Tsinghua University, Beijing 100084, China.

Tian Jian, Teng-Teng Chen and Lai-Sheng Wang are at the Department of Chemistry, Brown University, Providence, Rhode Island 02912, USA.

Correspondence to J.L. and L.S.W.
junli@tsinghua.edu.cn; lai-sheng_wang@brown.edu

doi:10.1038/s41570-017-0071
Published online 27 Sep 2017

1. Lipscomb, W. N. The boranes and their relatives. *Science* **196**, 1047–1055 (1977).
2. Kroto, H. W., Heath, J. R., O'Brian, S. C., Curl, R. F. & Smalley, R. E. C_{60}: Buckminsterfullerene. *Nature* **318**, 162–163 (1985).
3. Iijima, S. Helical microtubules of graphitic carbon. *Nature* **354**, 56–58 (1991).
4. Geim, A. K. & Novoselov, K. S. The rise of graphene. *Nat. Mater.* **6**, 183–191 (2007).
5. Oganov, A. R. *et al.* Ionic high-pressure form of elemental boron. *Nature* **457**, 863–867 (2009).
6. Boustani, I. & Quandt, A. Nanotubules of bare boron clusters: *ab initio* and density functional study. *Europhys. Lett.* **39**, 527–532 (1997).
7. Gindulytė, A., Lipscomb, W. N. & Massa, L. Proposed boron nanotubes. *Inorg. Chem.* **37**, 6544–6545 (1998).
8. Tang, H. & Ismail-Beigi, S. Novel precursors for boron nanotubes: the competition of two-center and three-center bonding in boron sheets. *Phys. Rev. Lett.* **99**, 115501 (2007).
9. Yang, X., Ding, Y. & Ni, J. *Ab initio* prediction of stable boron sheets and boron nanotubes: structure, stability, and electronic properties. *Phys. Rev. B* **77**, 041402 (2008).
10. Szwacki, N. G., Sadrzadeh, A. & Yakobson, B. I. B_{80} fullerene: an *ab initio* prediction of geometry, stability, and electronic structure. *Phys. Rev. Lett.* **98**, 166804 (2007).
11. Prasad, D. L. V. K. & Jemmis, E. D. Stuffing improves the stability of fullerenelike boron clusters. *Phys. Rev. Lett.* **100**, 165504 (2008).
12. Li, H. *et al.* Icosahedral B_{12}-containing core-shell structures of B_{80}. *Chem. Commun.* **46**, 3878–3880 (2010).
13. De, S. *et al.* Energy landscape of fullerene materials: a comparison of boron to boron nitride and carbon. *Phys. Rev. Lett.* **106**, 225502 (2011).
14. Li, F. Y. *et al.* B_{80} and $B_{101-103}$ clusters: remarkable stability of the core-shell structures established by validated density functionals. *J. Chem. Phys.* **136**, 074302 (2012).
15. Alexandrova, A. N., Boldyrev, A. I., Zhai, H. J. & Wang, L. S. All-boron aromatic clusters as potential new inorganic ligands and building blocks in chemistry. *Coord. Chem. Rev.* **250**, 2811–2866 (2006).
16. Sergeeva, A. P. *et al.* Understanding boron through size-selected clusters: structure, chemical bonding, and fluxionality. *Acc. Chem. Res.* **47**, 1349–1358 (2014).
17. Wang, L. S. Photoelectron spectroscopy of size-selected boron clusters: from planar structures to borophenes and borospherenes. *Int. Rev. Phys. Chem.* **35**, 69–142 (2016).
18. Hanley, L., Whitten, J. L. & Anderson, S. L. Collision-induced dissociation and *ab initio* studies of boron cluster ions: determination of structures and stabilities. *J. Phys. Chem.* **92**, 5803–5812 (1988).
19. Ruatta, S. A., Hanley, L. & Anderson, S. L. Dynamics of boron cluster ion reactions with deuterium: adduct formation and decay. *J. Chem. Phys.* **91**, 226–239 (1989).
20. Hintz, P. A., Ruatta, S. A. & Anderson, S. L. Interaction of boron cluster ions with water: single collision dynamics and sequential etching. *J. Chem. Phys.* **92**, 292–303 (1990).
21. Hintz, P. A., Sowa, M. B., Ruatta, S. A. & Anderson, S. L. Reactions of boron cluster ions (B_n^+, n = 2–24) with N_2O: NO versus NN bond activation as a function of size. *J. Chem. Phys.* **94**, 6446–6458 (1991).
22. Zhai, H. J., Wang, L. S., Alexandrova, A. N. & Boldyrev, A. I. Electronic structure and chemical bonding of B_5^- and B_5 by photoelectron spectroscopy and *ab initio* calculations. *J. Chem. Phys.* **117**, 7917–7924 (2002).
23. Alexandrova, A. N. *et al.* Structure and bonding in B_6^- and B_6: planarity and antiaromaticity. *J. Phys. Chem. A* **107**, 1359–1369 (2003).
24. Zhai, H. J., Alexandrova, A. N., Birch, K. A., Boldyrev, A. I. & Wang, L. S. Hepta- and octacoordinate boron in molecular wheels of eight- and nine-atom boron clusters: observation and confirmation. *Angew. Chem. Int. Ed.* **42**, 6004–6008 (2003).
25. Zhai, H. J., Kiran, B., Li, J. & Wang, L. S. Hydrocarbon analogues of boron clusters — planarity, aromaticity and antiaromaticity. *Nat. Mater.* **2**, 827–833 (2003).
26. Alexandrova, A. N., Boldyrev, A. I., Zhai, H. J. & Wang, L. S. Electronic structure, isomerism, and chemical bonding in B_7^- and B_7. *J. Phys. Chem. A* **108**, 3509–3517 (2004).
27. Kiran, B. *et al.* Planar-to-tubular structural transition in boron clusters: B_{20} as the embryo of single-walled boron nanotubes. *Proc. Natl Acad. Sci. USA* **102**, 961–964 (2005).
28. Sergeeva, A. P., Zubarev, D. Y., Zhai, H. J., Boldyrev, A. I. & Wang, L. S. A. Photoelectron spectroscopic and theoretical study of B_{16}^- and B_{16}^{2-}: an all-boron naphthalene. *J. Am. Chem. Soc.* **130**, 7244–7246 (2008).
29. Huang, W. *et al.* A concentric planar doubly π-aromatic B_{19}^- cluster. *Nat. Chem.* **2**, 202–206 (2010).
30. Sergeeva, A. P., Averkiev, B. B., Zhai, H. J., Boldyrev, A. I. & Wang, L. S. All-boron analogues of aromatic hydrocarbons: B_{17}^- and B_{18}^-. *J. Chem. Phys.* **134**, 224304 (2011).
31. Piazza, Z. A. *et al.* A photoelectron spectroscopy and *ab initio* study of B_{21}^-: negatively charged boron clusters continue to be planar at 21. *J. Chem. Phys.* **136**, 104310 (2012).
32. Sergeeva, A. P. *et al.* B_{22}^- and B_{23}^-: all-boron analogues of anthracene and phenanthrene. *J. Am. Chem. Soc.* **134**, 18065–18073 (2012).
33. Popov, I. A., Piazza, Z. A., Li, W. L., Wang, L. S. & Boldyrev, A. I. A combined photoelectron spectroscopy and *ab initio* study of the quasi-planar B_{24}^- cluster. *J. Chem. Phys.* **139**, 144307 (2013).
34. Piazza, Z. A. *et al.* A photoelectron spectroscopy and *ab initio* study of the structures and chemical bonding of the B_{25}^- cluster. *J. Chem. Phys.* **141**, 034303 (2014).
35. Li, W. L., Zhao, Y. F., Hu, H. S., Li, J. & Wang, L. S. [B_{30}^-]: a quasiplanar chiral boron cluster. *Angew. Chem. Int. Ed.* **53**, 5540–5545 (2014).
36. Li, W. L., Pal, R., Piazza, Z. A., Zeng, X. C. & Wang, L. S. B_{27}^-: appearance of the smallest planar boron cluster containing a hexagonal vacancy. *J. Chem. Phys.* **142**, 204305 (2015).
37. Wang, Y. J. *et al.* Observation and characterization of the smallest borosphere, B_{28}^- and B_{28}. *J. Chem. Phys.* **144**, 064307 (2016).
38. Li, H. R. *et al.* Competition between quasi-planar and cage-like structures in the B_{29}^- cluster: photoelectron spectroscopy and *ab initio* calculations. *Phys. Chem. Chem. Phys.* **18**, 29147–29155 (2016).
39. Luo, X. M. *et al.* B_{26}^-: the smallest planar boron cluster with a hexagonal vacancy and a complicated potential landscape. *Chem. Phys. Lett.* **683**, 336–341 (2017).
40. Hubert, H. *et al.* Icosahedral packing of B_{12} icosahedra in boron suboxide (B_6O). *Nature* **391**, 376–378 (1998).
41. White, M. A., Cerqueira, A. B., Whiteman, C. A., Johnson, M. B. & Ogitsu, T. Determination of phase stability of elemental boron. *Angew. Chem. Int. Ed.* **54**, 3626–3629 (2015).
42. Kawai, R. & Weare, J. H. Instability of the B_{12} icosahedral cluster: rearrangement to a lower energy structure. *J. Chem. Phys.* **95**, 1151–1159 (1991).
43. Boustani, I. Systematic *ab initio* investigation of bare boron clusters: determination of the geometry and electronic structures of B_n, n = 2–14. *Phys. Rev. B* **55**, 16426–16438 (1997).
44. Zubarev, D. Y. & Boldyrev, A. I. Developing paradigms of chemical bonding: adaptive natural density partitioning. *Phys. Chem. Chem. Phys.* **10**, 5207–5217 (2008).
45. Zubarev, D. Y. & Boldyrev, A. I. Comprehensive analysis of chemical bonding in boron clusters. *J. Comput. Chem.* **28**, 251–268 (2007).
46. Fowler, J. E. and Ugalde, J. M. The curiously stable B_{13}^+ cluster and its neutral and anionic counterparts: the advantage of planarity. *J. Phys. Chem. A* **104**, 397–403 (2000).
47. Boldyrev, A. I. & Wang, L. S. Beyond organic chemistry: aromaticity in atomic clusters. *Phys. Chem. Chem. Phys.* **18**, 11589–11605 (2016).
48. Piazza, Z. A. *et al.* Planar hexagonal B_{36} as a potential basis for extended single-atom layer boron sheets. *Nat. Commun.* **5**, 3113 (2014).
49. Li, W. L. *et al.* The B_{35} cluster with a double-hexagonal vacancy: a new and more flexible structural motif for borophene. *J. Am. Chem. Soc.* **136**, 12257–12260 (2014).
50. Chen, Q. *et al.* 2D B_{38}^- and B_{37}^- clusters with a double-hexagonal vacancy: molecular motifs for borophenes. *Nanoscale* **9**, 4550–4557 (2017).
51. Zhai, H. J. *et al.* Observation of an all-boron fullerene. *Nat. Chem.* **6**, 727–731 (2014).
52. Romanescu, C., Galeev, T. R., Li, W. L., Boldyrev, A. I. & Wang, L. S. Aromatic metal-centered monocyclic boron rings: Co©B_8^- and Ru©B_9^-. *Angew. Chem. Int. Ed.* **50**, 9334–9337 (2011).
53. Li, W. L. *et al.* Transition-metal-centered nine-membered boron rings: M©B_9 and M©B_9^- (M = Rh. Ir). *J. Am. Chem. Soc.* **134**, 165–168 (2012).
54. Galeev, T. R., Romanescu, C., Li, W. L., Wang, L. S. & Boldyrev, A. I. Observation of the highest coordination number in planar species: decacoordinated Ta©B_{10}^- and Nb©B_{10}^- anions. *Angew. Chem. Int. Ed.* **51**, 2101–2105 (2012).
55. Romanescu, C. *et al.* Experimental and computational evidence of octa- and nona-coordinated planar iron-doped boron clusters: Fe©B_8^- and Fe©B_9^-. *J. Organomet. Chem.* **721–722**, 148–154 (2012).
56. Romanescu, C., Galeev, T. R., Li, W. L., Boldyrev, A. I. & Wang, L. S. Transition-metal-centered monocyclic boron wheel clusters (M©B_n): a new class of aromatic borometallic compounds. *Acc. Chem. Res.* **46**, 350–358 (2013).
57. Popov, I. A., Jian, T., Lopez, G. V., Boldyrev, A. I. & Wang, L. S. Cobalt-centred boron molecular drums with the highest coordination number in the CoB_{16}^- cluster. *Nat. Commun.* **6**, 8654 (2015).
58. Jian, T. *et al.* Manganese-centered tubular boron cluster – MnB_{16}^-: a new class of transition-metal molecules. *J. Chem. Phys.* **144**, 154310 (2016).
59. Li, W. L. *et al.* Observation of a metal-centered B_2-Ta@B_{18}^- tubular molecular rotor and a perfect Ta@B_{20}^- boron drum with the record coordination number of twenty. *Chem. Commun.* **53**, 1587–1590 (2017).
60. Li, W. L. *et al.* The planar CoB_{18}^- cluster as a motif for metallo-borophenes. *Angew. Chem. Int. Ed.* **55**, 7358–7363 (2016).
61. Jian, T. *et al.* Competition between drum and quasi-planar structures in RhB_{18}^-: motifs for metallo-boronanotubes and metallo-borophenes. *Chem. Sci.* **7**, 7020–7027 (2016).
62. Zhang, H., Li, Y., Hou, J., Tu, K. & Chen, Z. FeB_6 monolayers: the graphene-like material with hypercoordinate transition metal. *J. Am. Chem. Soc.* **138**, 5644–5651 (2016).
63. Zhang, H., Li, Y., Hou, J., Du, A. & Chen, Z. Dirac state in the FeB_2 monolayer with graphene-like boron sheet. *Nano Lett.* **16**, 6124–6129 (2016).
64. Li, J. *et al.* Global minimum of two-dimensional FeB_6 and an oxidation induced negative Poisson's ratio: a new stable allotrope. *J. Mater. Chem. C* **4**, 9613–9621 (2016).
65. Li, J. *et al.* Voltage-gated spin-filtering properties and global minimum of planar MnB_6, and half-metallicity and room-temperature ferromagnetism of its oxide sheet. *J. Mater. Chem. C* **4**, 10866–10875 (2016).
66. Mannix, A. J. *et al.* Synthesis of borophenes: anisotropic, two-dimensional boron polymorphs. *Science* **350**, 1513–1516 (2015).
67. Feng, B. *et al.* Experimental realization of two-dimensional boron sheets. *Nat. Chem.* **8**, 563–568 (2016).
68. Zhao, J. *et al.* B_{28}: the smallest all-boron cage from an *ab initio* global search. *Nanoscale* **7**, 15086–15090 (2015).
69. Romanescu, C., Sergeeva, A. P., Li, W. L., Boldyrev, A. I. & Wang, L. S. Planarization of B_7^- and B_{12}^- clusters by isoelectronic substitution: AlB_6^- and AlB_{11}^-. *J. Am. Chem. Soc.* **133**, 8646–8653 (2011).
70. Romanescu, C., Harding, D. J., Fielicke, A. & Wang, L. S. Probing the structures of neutral boron clusters using infrared/vacuum ultraviolet two color ionization: B_{11}, B_{16}, and B_{17}. *J. Chem. Phys.* **137**, 014317 (2012).
71. Czekner, J., Cheung, L. F. & Wang, L. S. Probing the structures of neutral B_{11} and B_{12} using high resolution photoelectron imaging of B_{11}^- and B_{12}^-. *J. Phys. Chem. C* **121**, 10752–10759 (2017).
72. Oger, E. *et al.* Boron cluster cations: transition from planar to cylindrical structures. *Angew. Chem. Int. Ed.* **46**, 8503–8506 (2007).
73. Boustani, I. Systematic LSD investigation on cationic boron clusters: B_n^+ (n = 2–14). *Int. J. Quantum Chem.* **52**, 1081–1111 (1994).
74. Ricca, A. & Bauschlicher, C. W. The structure and stability of B_n^+ clusters. *Chem. Phys. Lett.* **208**, 233–242 (1996).
75. Fagiani, M. R. *et al.* Structure and fluxionality of B_{13}^+ probed by infrared photodissociation spectroscopy. *Angew. Chem. Int. Ed.* **56**, 501–504 (2017).
76. Martinez-Guajardo, G. *et al.* Unraveling phenomenon of internal rotation in B_{13}^+ through chemical bonding analysis. *Chem. Commun.* **47**, 6242–6244 (2011).
77. Boustani, I., Quandt, A., Hernández, E. & Rubio, A. New boron based nanostructured materials. *J. Chem. Phys.* **110**, 3176–3185 (1999).

78. Evans, M. H., Joannopoulos, J. D. & Pantelides, S. T. Electronic and mechanical properties of planar and tubular boron structures. *Phys. Rev. B* **72**, 045434 (2005).
79. Kunstmann, J. & Quandt, A. Broad boron sheets and boron nanotubes: an *ab initio* study of structural, electronic, and mechanical properties. *Phys. Rev. B* **74**, 035413 (2006).
80. Lau, K. C. & Pandey, R. Stability and electronic properties of atomistically-engineered 2D boron sheets. *J. Phys. Chem. C* **111**, 2906–2912 (2007).
81. Penev, E. S., Bhowmick, S., Sadrzadeh, A. & Yakobson, B. I. Polymorphism of two-dimensional boron. *Nano Lett.* **12**, 2441–2445 (2012).
82. Wu, X. *et al.* Two-dimensional boron monolayer sheets. *ACS Nano* **6**, 7443–7453 (2012).
83. Liu, Y., Penev, E. S. & Yakobson, B. I. Probing the synthesis of two-dimensional boron by first-principles computations. *Angew. Chem. Int. Ed.* **52**, 3156–3159 (2013).
84. Liu, H., Gao, J. & Zhao, J. From boron cluster to two-dimensional boron sheet on Cu(111) surface: growth mechanism and hole formation. *Sci. Rep.* **3**, 3238 (2013).
85. Zhang, Z., Yang, Y., Gao, G. & Yakobson, B. I. Two-dimensional boron monolayers mediated by metal substrates. *Angew. Chem. Int. Ed.* **54**, 13022–13026 (2015).
86. Xu, S., Zhao, Y., Liao, J., Yang, X. & Xu, H. The nucleation and growth of borophene on the Ag(111) surface. *Nano Res.* **9**, 2616–2622 (2016).
87. Zhang, Z. *et al.* Substrate-induced nanoscale undulations of borophene on silver. *Nano Lett.* **16**, 6622–6627 (2016).
88. Mannix, A. J., Kiraly, B., Hersam, M. C. & Guisinger, N. P. Synthesis and chemistry of elemental 2D materials. *Nat. Rev. Chem.* **1**, 0014 (2017).
89. Shu, H., Li, F., Liang, P. & Chen, X. Unveiling the atomic structure and electronic properties of atomically thin boron sheets on an Ag(111) surface. *Nanoscale* **8**, 16284–16291 (2016).
90. Zabolotskiy, A. D. & Lozovik, Y. E. Strain-induced pseudomagnetic field in the Dirac semimetal borophene. *Phys. Rev. B* **94**, 165403 (2016).
91. Sun, H. Li, Q. & Wan, X. G. First-principles study of thermal properties of borophene. *Phys. Chem. Chem. Phys.* **18**, 14927–14932 (2016).
92. Zhang, Z., Yang, Y., Penev, E. S. & Yakobson, B. I. Elasticity, flexibility, and ideal strength of borophenes. *Adv. Funct. Mater.* **27**, 1605059 (2017).
93. Zhao, Y. Zeng, S. & Ni, J. Phonon-mediated superconductivity in borophenes. *Appl. Phys. Lett.* **108**, 242601 (2016).
94. Penev, E. S., Kutana, A. & Yakobson, B. I. Can two-dimensional boron superconduct? *Nano Lett.* **16**, 2522–2526 (2016).
95. Xiao, R. C. *et al.* Enhanced superconductivity by strain and carrier-doping in borophene: a first principles prediction. *Appl. Phys. Lett.* **109**, 122604 (2016).
96. Gao, M., Li, Q. Z., Yan, X. W. & Wang, J. Prediction of phonon-mediated superconductivity in borophene. *Phys. Rev. B* **95**, 024505 (2017).
97. Galeev, T. R., Romanescu, C., Li, W. L., Wang, L. S. & Boldyrev, A. I. Valence isoelectronic substitution in the B_8^- and B_9^- molecular wheels by an Al dopant atom: umbrella-like structures of AlB_7^- and AlB_8^-. *J. Chem. Phys.* **135**, 104301 (2011).
98. Li, W. L., Romanescu, C., Piazza, Z. A. & Wang, L. S. Geometrical requirements for transition-metal-centered aromatic boron wheels: the case of VB_{10}^-. *Phys. Chem. Chem. Phys.* **14**, 13663–13669 (2012).
99. Li, W. L. *et al.* On the way to the highest coordination number in the planar metal-centred aromatic $Ta@B_{10}^-$ cluster: evolution of the structures of TaB_n^- (n = 3 – 8). *J. Chem. Phys.* **139**, 104312 (2013).
100. Popov, I. A., Li, W. L., Piazza, Z. A., Boldyrev, A. I. & Wang, L. S. Complexes between planar boron clusters and transition metals: a photoelectron spectroscopy and *ab initio* study of CoB_{12}^- and RhB_{12}^-. *J. Phys. Chem. A* **118**, 8098–8105 (2014).
101. Li, W. L. *et al.* Hexagonal bipyramidal $Ta_2B_6^{-/0}$ clusters: B_6 rings as structural motifs. *Angew. Chem. Int. Ed.* **53**, 1288–1292 (2014).
102. Robinson, P. J., Zhang, X., McQueen, T., Bowen, K. H. & Alexandrova, A. N. SmB_6^- cluster anion: covalency involving *f* orbitals. *J. Phys. Chem. A* **121**, 1849–1854 (2017).
103. Chen, T. T. *et al.* PrB_7^-: A praseodymium-doped boron cluster with a Pr(II) center coordinated by a doubly aromatic planar η^7-B_7^{3-} ligand. *Angew. Chem. Int. Ed.* **56**, 6916–6920 (2017).
104. Romanescu, C., Galeev, T. R., Li, W. L., Boldyrev, A. I. & Wang, L. S. Geometric and electronic factors in the rational design of transition-metal-centered boron molecular wheels. *J. Chem. Phys.* **138**, 134315 (2013).
105. Xu, C., Cheng, L. J. & Yang, J. L. Double aromaticity in transition metal centered double-ring boron clusters $M@B_{2n}$ (M = Ti, Cr, Fe, Ni, Zn; n = 6, 7, 8). *J. Chem. Phys.* **141**, 124301 (2014).
106. Tam, N. M., Pham, H. T., Duong, L. V., Pham-Ho, M. P. & Nguyen, M. T. Fullerene-like boron clusters stabilized by an endohedrally doped iron atom: B_nFe with n = 14, 16, 18 and 20. *Phys. Chem. Chem. Phys.* **17**, 3000–3003 (2015).
107. Zhao, Y., Xin, C. & Li, J. TGMin: a global-minimum structure search program based on a constrained basin-hopping algorithm. *Nano Res.* **10**, 3407–3420 (2017).
108. Chen, X., Zhao, Y. F., Wang, L. S. & Li, J. Recent progresses of global minimum searches of nanoclusters with a constraint basin-hopping algorithm in the TGMin program. *Comput. Theor. Chem.* **1107**, 57–65 (2017).
109. Carenco, S., Portehault, D., Boissiere, C., Mezailles, N. & Sanchez, C. Nanoscaled metal borides and phosphides: recent developments and perspectives. *Chem. Rev.* **113**, 7981–8065 (2013).
110. Rastgou, A., Soleymanabadi, H. & Bodaghi, A. DNA sequencing by borophene nanosheet via an electronic response: a theoretical study. *Microelectron. Eng.* **169**, 9–15 (2017).
111. Garcia-Fuente, A., Carrete, J., Vega, A. & Gallego, L. J. What will freestanding borophene nanoribbons look like? An analysis of their possible structures, magnetism and transport properties. *Phys. Chem. Chem. Phys.* **19**, 1054–1061 (2017).
112. Feng, B. *et al.* Dirac fermions in borophene. *Phys. Rev. Lett.* **118**, 096401 (2017).
113. Liu, X. *et al.* Self-assembly of electronically abrupt borophene/organic lateral heterostructures. *Sci. Adv.* **3**, e1602356 (2017).

Acknowledgements
The experimental work on size-selected boron clusters at Brown University was supported by the US National Science Foundation (Grant No. CHE-1263745). The theoretical work done at Tsinghua University was supported by the National Key Basic Research Special Funds (Grant No. 2013CB834603) and the National Natural Science Foundation of China (Grant Nos 21433005, 91426302 and 21590792) of China. The calculations were performed using supercomputers at the Computer Network Information Center, Chinese Academy of Sciences, Tsinghua National Laboratory for Information Science and Technology, and Guangzhou Tianhe-2 Supercomputing Center.

Competing interests statement
The authors declare no competing interests.

How to cite this article
Li, W.-L. *et al.* From planar boron clusters to borophenes and metalloborophenes. *Nat. Rev. Chem.* **1**, 0071 (2017).